Heliyon 10 (2024) e32420

Contents lists available at ScienceDirect

Heliyon

journal homepage: www.cell.com/heliyon

Research article

Liquid foaming of TPU with Methylal

Lorenzo Miele [a,b,1], Emilia Di Lorenzo [a,b,1], Céline Guissart [c], Ernesto Di Maio [a,b,*]

[a] Dipartimento di Ingegneria Chimica, dei Materiali e della Produzione Industriale, University of Naples Federico II, P.le Tecchio 80, 80125, Naples, Italy
[b] foamlab, University of Naples Federico II, P.le Tecchio 80, 80125, Naples, Italy
[c] Lambiotte et Compagnie S.A., Avenue des Aubépines, 18, B-1180, Brussels, Belgium

ARTICLE INFO

Keywords:
Liquid foaming
Dimethoxymethane
TPU
Blowing agents
Methylal

ABSTRACT

This work investigates the peculiarities of using a liquid blowing agent, namely dimethoxymethane (Methylal) to foam a thermoplastic polyurethane (TPU) in the laboratory practice of batch foaming equipment. We preliminarily measured thermodynamic properties of the polymer/gas system relevant to foaming, namely the vapor-liquid pressures at the TPU foaming temperatures. Three different paths were then explored for foaming. First, we used Methylal under its liquid-vapor equilibrium condition, in which both liquid and vapor are present. Secondly, we used Methylal in the liquid state to experiment with liquid foaming strategies. We have observed specific aspects, details, and issues related to the use of liquid blowing agents and devised strategies to deal with them. Finally, we used Methylal as a co-blowing agent together with CO_2. In all cases, we examined the impact of pressure, pressure drop rate, and temperature on foam density and morphology.

Overall, liquid foaming has proven to be a viable technique and Methylal an effective blowing agent, especially in cooperation with other gaseous blowing agents, where it significantly improves the expansion ratio of the final product.

1. Introduction

Thermoplastic elastomers (TPE) are currently of great interest in the industry due to their high ductility, resilience, and, most importantly, their environmentally friendly nature [1–3]. In fact, they are preferred to thermosetting elastomers because they are fully recyclable [4]. Thermoplastic polyurethanes (TPU), in particular, are a class of linear segmented block copolymers having hard segments (HS) and soft segments (SS). HS act as multifunctional tie points functioning both as physical crosslinks and reinforcement fillers, while SS form an elastomeric matrix that accounts for the large strain elasticity [3]. The advantage of this peculiar structure is that, by simply varying the SS-HS ratio, the physical properties of the TPU can be tuned [5]. These characteristics make TPU suitable for a wide range of applications, such as supercapacitor, shape memory, automotive parts, and sensor [6], but also for packaging, sportswear, insulation, and construction in the peculiar case of TPU foams. In fact, TPU foams present a series of non-trivial advantages compared to their unfoamed counterparts, including light weight, low thermal conductivity, high strength-to-weight ratio, and dissipation of impact energy, among others [7].

* Corresponding author.
E-mail addresses: lorenzo.miele@unina.it (L. Miele), emilia.dilorenzo2@unina.it (E. Di Lorenzo), c.guissart@lambiotte.com (C. Guissart), edimaio@unina.it (E. Di Maio).
[1] Contributed equally to this work.

https://doi.org/10.1016/j.heliyon.2024.e32420
Received 11 December 2023; Received in revised form 24 March 2024; Accepted 4 June 2024
Available online 6 June 2024

Thermoplastic polymeric foams are traditionally produced with two different techniques: chemical foaming and physical foaming [8]. Chemical foaming relies on a chemical reaction to deliver a blowing agent to the polymer; the reactant can be easily admixtured to the polymer during compounding but is often unable to give low-density foams [9–11]. Physical foaming exploits the introduction of a physical blowing agent (PBA); it requires a special feeding system in the final processing stage, but can push the limit of the specific polymer to the low-density end [12–14]. As a result of the gaseous physical state of the PBA during the foaming process, physical foaming is also known as gas foaming [8]. Gas foaming is common to different technologies, namely batch [15], extrusion [16], injection molding [17] and steam chest molding [18]. For this study we focused on batch foaming, as it is the simplest process for making foams on the laboratory scale, where small sample sizes, in the order of a few grams, can be utilized. This technique is based on the use of a thermoregulated pressure vessel in which the polymer is placed and the PBA is subsequently injected at a certain pressure to allow sorption into the polymer. After a polymer/gas solution is obtained, phase separation occurs by increasing the temperature or quenching the pressure [8]. This technique is not only very versatile in terms of equipment, but also offers the possibility of a fine control of foaming variables over a wide range, which in turn provides a good control of the final density and cellular morphology of the foam.

The main process parameters are directly suggested by the classical nucleation theory [19] and include the gas concentration before foaming (in batch foaming, it is related to the solubilization pressure, if equilibrium conditions are reached in the sorption process) and the foaming temperature. This set of process variables is completed by the pressure release history $P(t)$, which can dramatically influence the foaming outcome, especially in terms of the final foam morphology. As a consequence, a comprehensive analysis of $P(t)$ is essential for gaining deeper insights into the complex dynamics governing foam formation and structure development. In the simplest scenario, $P(t)$ is characterized solely by its maximum rate, referred to as the pressure drop rate (*PDR*) [20,21].

On top of that, selection of the PBA is pivotal within this process. In fact, the chemophysical properties of the PBA determine its solubility and diffusivity in the polymer, and the volumetric, interfacial and rheological properties of the polymer/gas solution [22,23]. Consequently, the choice of one PBA over the other represents a powerful tool for tuning foam properties, in terms of both foam morphology and foam density. Possible PBAs for gas foaming include gases like carbon dioxide and nitrogen, in subcritical or supercritical conditions, but also low boiling point liquids, such as pentane, butane, and hydrochlorofluorocarbons [7,24,25]. Among these, the use of carbon dioxide as a PBA has gained a lot of interest over the years and has long been established thanks to its properties; in fact, it is not considered a contaminating agent, it does not leave toxic residues in the final product, and it does not cause safety issues. However, the production of low-density foams with CO_2 still remains challenging due to its low solubility and high diffusivity [22].

To overcome these problems, mixtures of CO_2 with other BAs have also been tested. In this case, to achieve the best possible outcome, it is crucial to separately study the role of each PBA during the foaming process with respect to the solubility, foaming kinetics, and setting mechanism, and then design the optimal PBA mixture/recipe [22,26].

The majority of studies with co-blowing agents deal with the extrusion process. Salerno et al. [27] used mixtures of CO_2 and ethyl lactate (EL) to foam polyesters, while Tsivintzelis et al. [28] and Gendron et al. [26] used mixtures of CO_2 and ethanol for foaming of polycaprolactone (PCL) and polystyrene (PS), respectively. Similarly, in a different work [29], extruded PS foams were prepared by using a mixture of CO_2 and 2-ethyl hexanol, which acted as an efficient additional plasticizer. Reports on the use of CO_2/H_2O mixtures are also present, like in the works by Zhao et al. [30] and Zhang et al. [31]. The blending of CO_2 with an alcohol or a ketone was also proposed for extruded PS sheets of high compressive strength [32]. In all listed cases, improved foam morphology uniformity and improved foam density were reported. Nevertheless, studies on extrusion foaming cannot be easily transferred to batch foaming. In fact, PDR in extrusion is dictated by the shape of the die and the rheology of the polymer/PBA solution.

Fewer studies were carried out on batch foaming. The use of CO_2/toluene mixtures [33] and n-pentane (nC5)/CO_2 and cyclopentane(cC5)/CO_2 mixtures [34] on PS was reported [33,34]. The results suggest that pre-impregnating PS with a blowing agent in its liquid state before the CO_2 batch foaming enhances CO_2 solubility and lowers the glass transition temperature (T_g) of the system, giving higher foam porosity, without modifying the polymer. Similarly, Xiaoqin et al. [35] observed that PP foams blown with a CO_2/n-pentane mixture in batch foaming exhibit a lower foaming temperature, a higher expansion ratio, and a lower cell density relative to those blown with CO_2 alone because of the different gas solubilities of the blowing agents. As an alternative, the use of low boiling point liquids alone, like pentane and butane, has also been tested, even if no direct comparison with the other mentioned techniques has ever been reported. In the work of Tuladhar and Mackley [36], pentane is impregnated in the polymer melt and then allowed to nucleate and evaporate through a rapid pressure drop to induce phase separation. Effect of foaming parameters such as impregnation time, temperature and sorption pressure on the foaming dynamics of PS and styrene-methyl methacrylate copolymer were studied using pentane as the blowing agent by Salejova and Kosek [37] and Azimi et al. [38,39]. On the same note, Mostafa et al. [40] studied experimentally and theoretically PS/n-pentane batch foaming. Despite the valuable insights provided by the above mentioned studies, there remains a notable gap in our understanding regarding the criticalities in using a substance in its liquid state as a blowing agent. In this work we will address the non-trivial aspects of using such a technique, with a special focus on the occurrence of phase transition, from liquid to vapor, and vice versa, that modifies the dynamics of the process.

The possibility of extending the current knowledge about the use of liquid blowing agents in the context of foaming thermoplastic polymers, and TPU in particular, is here faced. Indeed, to the best of our knowledge, no study reports in detail the technological implications of using a BA in its liquid state, and the pivotal effect of *PDR* is often neglected.

Several methods have been reported in the literature to prepare TPU foams, including batch foaming [41], and many blowing agents have been used, such as the environmentally friendly CO_2 and N_2, but also butane, azodicarbonamide and $NaHCO_3$ [24]. Despite this, the use of liquid blowing agent in TPU foaming is not yet an established practice. In this sense, we remark the work by Hossieny et al. [25], where butane as blowing agent in its liquid state was used to produce microcellular TPU foams. Here, chemical

interaction of the liquid with the polymer and consequent redistribution of the hard segments of TPU were exploited through production of crystalline domains that act as nucleating agents.

Dimethoxymethane (Methylal) is a low molecular weight substance with a low boiling point (42.3 °C) [42]. It is used predominantly as a solvent and as a building block in organic syntheses [43]. It has been used as a blowing agent for thermosetting polyurethane-based foams, alone or in mixtures with 1,1,1,3,3-pentafluoropropane, giving products with non-uniform cellular structures, and inadequate thermal insulating performances and compression strengths have been reported [44,45]. The use of Methylal as the PBA for the production of any thermoplastic polymer foams has never been reported to this day.

In the present article, Methylal is used as a PBA in TPU foaming. Because of the thermodynamic properties of the adopted PBA, and its liquid physical state at the temperatures suitable for TPU foaming processing, a proper design of the foaming experiments is at hand. These are detailed and addressed in the study. Preliminary tests are performed on Methylal to study its physical properties under conditions suitable for TPU foaming. Foaming tests with Methylal as sole PBA and as a co-blowing agent with CO_2 and N_2 are performed to demonstrate its potential to adjust the resulting foam features, with the aim of providing improved foaming performance. The possibility of exploiting Methylal to address specifical TPU criticalities, such as its stability problems [46,47], is presented.

2. Experimental

2.1. Materials

Commercial TPU (Elastollan 45A 12 P, BASF, Ludwigshafen, Germany) was used in the form of pellets, shore hardness 46A, and density 1180 kg/m^3. Before use, the as received TPU was dried in a vacuum oven at 80.0 °C for 3 h and then stored under vacuum. CO_2 and N_2 (purity 99.99%) were supplied by SOL S.p.A. (Monza, Italy). Methylal (Dimethoxymethane, $H_3COCH_2OCH_3$, CAS. No. 109-87-5, $M_W = 76.1$) was supplied by Lambiotte & CIE S.A. (Brussels, Belgium).

2.2. Experimental setup

Physical foaming of TPU beads was performed by a custom pressure vessel designed to allow (a) a fine-tuning of the foaming variables (temperature of the expanding matter, pressure and *PDR*, the latter, especially toward high values), (b) introduction of liquid PBA, (c) fast extraction of the foamed sample, and (d) the possibility of visually inspecting the foaming experiment.

To this end, as illustrated in Fig. 1, the pressure vessel was equipped with a total of four connections/ports, as described in detail elsewhere [48].

A Pt100 temperature sensor (positioned as close to the sample as possible) is installed through the first port to allow temperature control. The second port is connected through a "T" fitting to both a pressure transducer and a manifold for the introduction of the PBA (the manifold is connected to the PBA dosing system and a vacuum pump, necessary for pre-treatment of the beads). The third port is used for the introduction of the beads and is then closed with a 1/2" NPT sapphire window (Precision Sapphire Technologies Ltd., Vilnius, Lithuania) to allow visual observation of the experiments. Finally, the fourth port connects to a ball valve (10–80 NFH ball valve, High Pressure Equipment Company, Erie, USA), activated by an electromechanical actuator, and allows fast and reproducible release of the PBA. This port is also used to extract the samples rapidly, as the foamed TPU beads are small enough to be dragged by fluid flow to the exit [48]. A total of five TPU beads is tested simultaneously in the internal compartment of the vessel to ensure the

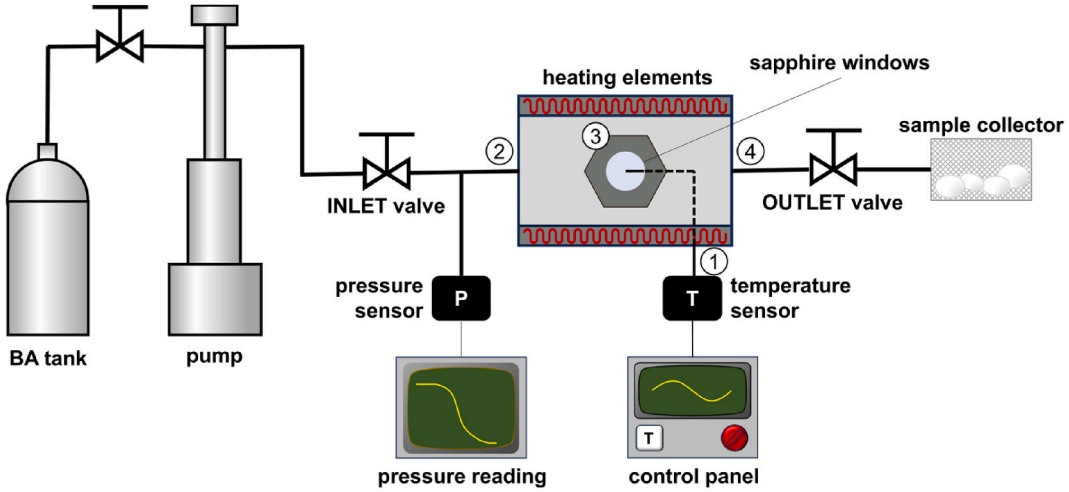

Fig. 1. Schematic of the experimental setup used for the liquid and gas foaming experiments where: (1) indicates the port connected to the thermocouple; (2) indicates the port connected to the pressure sensor and the manifold; (3) indicates the viewing port, with a sapphire window, and (4) indicates the port used for the release of the PBA and concomitant expulsion of the samples.

distribution of the data acquired from each experiment.

The setup thus described works with gaseous and liquid blowing agents: when using a gaseous blowing agent (CO_2 and N_2, namely), the second port is connected to the gas dosing system, while when using a liquid blowing agent (Methylal, namely), it is connected to a high pressure syringe pump (model 500D, Teledyne ISCO Syringe Pumps, Thousand Oaks, USA) that is capable of dosing the liquid inside the vessel at the desired pressure. The liquid is loaded in the syringe pump through a tube inserted directly into the Methylal bottle, while the piston of the pump is retracted to suck the liquid.

2.3. Liquid and gas foaming experiments

Foaming experiments were conducted in three ways, namely: (i) liquid-vapor foaming, (ii) liquid foaming and (iii) gas foaming, depending on the physical state of the PBA and desired foaming conditions. The procedures are described below.

(i) The liquid-vapor foaming technique requires a PBA under liquid-vapor equilibrium conditions at foaming temperatures. In this case, the foaming pressure is the vapor pressure. The pre-treated TPU beads are inserted into the vessel and kept under vacuum at 80.0 °C for 1 h to remove the humidity absorbed by the granules during handling. The liquid blowing agent (Methylal) is then injected into the vessel at ambient pressure with a pipette through port two. After pressure-tight closing the vessel, the desired temperature is imposed. At the given temperature, thermodynamic equilibrium and the vapor pressure are reached if any liquid is present. After a solubilization time of 30 min, foaming is performed through a quick pressure drop at a controlled *PDR*. Here, the solubilization pressure corresponds with the vapor pressure. As a consequence, it is regulated through the choice of the temperature and decoupling of these two process parameters is not possible. For this same reason, this method allows only for low-pressure foaming, as the temperatures suitable for TPU foaming correspond to equilibrium vapor pressures lower than 10 bar (see sections 2.5 and 3.1).

(ii) In the liquid foaming technique, pressures are higher than the vapor pressure and the PBA is in the liquid state. The pre-treated TPU beads are inserted in the vessel and kept under vacuum at 80.0 °C for 1 h to remove humidity absorbed by granules during handling. The liquid blowing agent is then injected into the vessel with a syringe pump that is capable of imposing a desired pressure. After a solubilization time of 30 min, foaming is performed through a quick pressure drop at a controlled PDR. With this method, pressures up to 90 bar were reached.

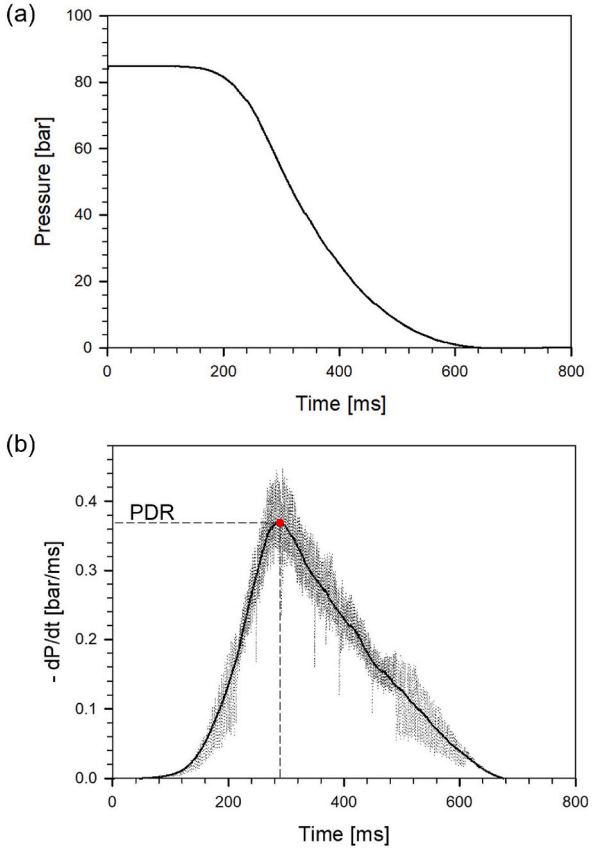

Fig. 2. (a) Pressure reduction over time; (b) moving average of central derivative of $P(t)$ (black) and central derivative of $P(t)$ (gray).

(iii) The gas foaming technique requires a gaseous PBA. In this case, TPU pellet pre-treatment was the same as described in the previous case, but the pressure of the gaseous BA, namely CO_2 and N_2, is here regulated with a pump (Nex10 Liquid Carbon Dioxide Pump, Supercritical Fluid Technologies INC., Newark, US) directly connected to the relative gas tank. The solubilization time was 1 h instead of 30 min depending on the different diffusivities of the gases with respect to liquid Methylal. This same technique is also used to perform experiments with mixtures of liquid and gaseous blowing agents (CO_2 and Methylal mixture as well as N_2 and Methylal mixture). The preparation of the mixture is ensured by preliminary placing the pre-treated beads in a Methylal bath for at least 1 h before being inserted into the vessel.

2.4. Pressure drop rate measurement

An important control variable of the physical foaming method through pressure quench is *PDR* [49]. The characteristic time of the pressure drop is very short ($\tau_{PD} \sim 1000$ ms), thus a very high data acquisition rate is required. For this reason we measured the *PDR* through a PLC (SIMATIC S7-1200 CPU, Siemens, Munich, Germany) with a sampling rate $\tau_m \sim 1$ ms. This device registers the pressure values over time and provides as output a curve $P(t)$. The shape of this curve depends on test conditions and PBA nature. We used numerical methods to analyze the $P(t)$ curve and calculate the largest time derivative ($:= PDR$). First, we applied a moving average to smooth out the short-term fluctuations and highlight the longer term trend. The average involves 99 data points corresponding to a time interval (10 ms) that is two orders of magnitude smaller than the characteristic time of the pressure reduction (1000 ms). Then we applied the midpoint method to evaluate the derivative. This derivative operation amplifies the noise of the signal, thus a moving average (99 points) was again applied to smooth out the data. At the end of the processing, *PDR* was evaluated as the highest peak value of the $-dP/dt$ curve. A visual representation of this evaluation is shown in Fig. 2. This method proved to be the most efficient among all the tested ones for *PDR* evaluation (namely, line interpolation and curve fitting). The main advantage lies in the independence from a mathematical model to describe the $P(t)$ curve and from the human bias (on the interval in which the curve is interpolated). Also, amongst the advantages it stood out that we could apply this method to any $P(t)$ curve, even when non trivial shapes were detected.

2.5. Liquid-vapor equilibrium methylal

The vapor pressure of Methylal was investigated in order to avail data useful for foaming tests [50,51]. The experiments were conducted in the above-mentioned mini-batch vessel, which acts as a closed system. For the scope, this was equipped with a valve for the injection of Methylal in its liquid state. We used the following procedure. First, we filled the mini-batch with Methylal in its liquid state at ambient temperature. Then we increased the temperature to a predefined value (that is, 96.0, 118.0, 135.0 and 154.0 °C) and we waited until the gas-liquid equilibrium was reached, that is, when the temperature and pressure of the system remained stable for at least 1 h, with an error of 5%. The pressure value at each condition was recorded as the vapor pressure of Methylal at that specific temperature value. For all measurements, the temperature sensor happened to be submerged in the liquid. Equilibrium parameters value thus found were used as temperature-pressure conditions to perform liquid-vapor foaming experiments with Methylal. It is important to note that, before experiments, the cell was evacuated with a vacuum pump, while during the experiments, the sapphire window was used to check the presence of liquid inside the vessel.

2.6. TPU foam characterization

Density measurements, optical microscopy, and scanning electron microscopy were used to characterize the TPU samples after foaming. The density measurements were performed using a density kit mounted on a laboratory balance (MS104S/01, Mettler Toledo, Columbus, Ohio). The test standard used was ASTM D792-00: by measuring the weight of the foamed sample both in air (w_{air}) and in water (w_{water}), density of the sample is calculated as:

$$\rho = \frac{w_{air}}{w_{air} - w_{water}} \times \rho_{water} \tag{1}$$

For each sample, the density was calculated as the mean of five replicates. Every measurements was made immediately after foaming. Days after foaming, as also seen elsewhere [46,52], shrinkage of the beads was observed, but this will not be explored in detail in the present work.

An optical microscope (Stemi 508, Zeiss, Oberkochen, Germany) was used to observe the morphology of TPU foams obtained with the liquid foaming technique, while a scanning electron microscope (SEM Merlin VP, Zeiss, Oberkochen, Germany) was used to observe the morphology of the TPU foams obtained with the gas foaming technique, because they had a much finer morphology. To prepare the optical microscopy and SEM specimen, TPU foams were cut using an ultrathin stainless steel blade. In the case of SEM specimens, the cross section was then coated with a thin layer of gold using a sputter coater (Auto Sputter Coater, Agar Scientific, Essex, UK). In the case of SEM, a ten days delay between the foaming experiment and the characterization caused shrinkage to occur before the images were collected. Again, this aspect will not be discussed in detail in the present work. Weight measurements of TPU beads were also performed before and after foaming to collect additional information.

2.7. Solubility and swelling measurements

Information about the interaction of Methylal with TPU in terms of solubility and consequent swelling of the beads was collected by measuring the weight and volume of the beads before and after immersion in a Methylal bath. Weight measurements were performed with a Mettler Toledo laboratory balance and then used to evaluate solubility in terms of weight fraction, x_e, at equilibrium:

$$x_e = \frac{w_{beads}|_{t=\infty} - w_{beads}|_{t=0}}{w_{beads}|_{t=0}} \tag{2}$$

Where $w_{b_{eads}l}|_{t=\infty}$ is the weight of the beads after the immersion process and $w_{beads}|_{t=0}$ is the weight of the beads before the immersion process. Volume measurements were made by taking pictures of the beads at the times of interest and then analyzing them with ImageJ [53]. In each image, the "edge detection" and "profile integration" commands were used to detect the edges of the beads and subsequently derive the beads volume values. From these data, swelling, *Sw*, was evaluated as:

$$Sw = \frac{V|_{t=\infty} - V|_{t=0}}{V|_{t=0}} \tag{3}$$

Where $V|_{t=0}$ and $V|_{t=\infty}$ are the volume before and after immersion in Methylal.

3. Results and discussion

First, we will explore the thermodynamic properties of Methylal, the interaction of Methylal with TPU, specifically in terms of solubility and swelling, and the peculiar shape of the pressure drop history noticed while performing the foaming experiments. Then, we will thoroughly describe the results of the foaming experiments, for each of the three ways described in subsection 2.3: (i) liquid-vapor and (ii) liquid foaming experiments with Methylal alone and (iii) gas-foaming experiments with CO_2 and Methylal as co-blowing agents. In each case, effect of process parameters and foam morphology will be presented. The results of foaming experiments with N_2 alone and N_2 and Methylal as co-blowing agents will not be presented because, in the same conditions used for CO_2, no foaming was detected.

3.1. Liquid-vapor equilibrium methylal

The experimental results of the investigation of the thermodynamic properties of Methylal are shown in Fig. 3. In the range mentioned above, the vapor pressure varies from 4.4 to 15.4 bar, consistent with data from the literature [50,51]. We can see that the maximum pressure at which we can use Methylal at equilibrium is approximately 9 bar, as imposed by the maximum temperature at which the polymer can be processed (polymer melting temperature). As a consequence, the use of Methylal at higher pressures is possible only in the fully liquid state.

3.2. Solubility and swelling

To test the interaction between Methylal and TPU, solubility measurements were performed. This preliminary study is fundamental to our research because it allows us to understand Methylal potential as a PBA (high solubility is required for any substance to be considered a good PBA). Under ambient conditions, $x_e = 0.493$, while at 5.5 bar and 116.6 °C, $x_e = 0.744$.

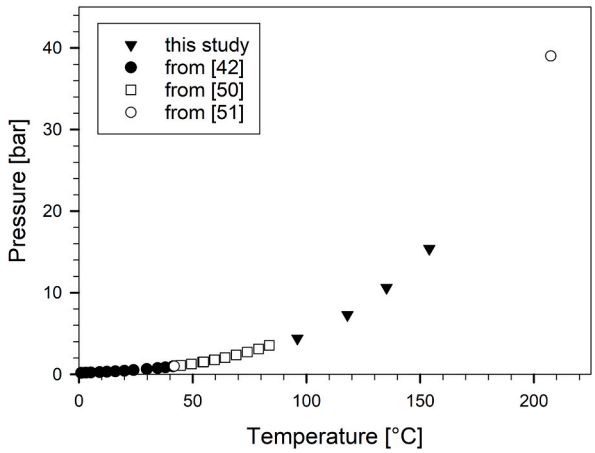

Fig. 3. Vapor pressures of Methylal.

These values are high enough to demonstrate that Methylal has the potential to be a good PBA. In fact they are orders of magnitude higher than the typical solubility values of gaseous blowing agents (namely N_2 and CO_2) in TPU [23].

Methylal also shows a strong swelling ability in its liquid state, with $Sw = 69.8\%$ at 45.0 bar and 131.8 °C. Here, the high amount of swelling is related to the high solubility of Methylal in TPU. Finally, the weight of the samples before and after foaming were recorded and an 11.5% w/w weight loss after contact with Methylal was observed. In fact, it is possible that Methylal extracts low molecular weight fractions or additives from the granules.

This hypothesis was corroborated by the in-situ observation of the liquid foaming experiments, at the end of which some material, itself foamed during the pressure release, could be seen on the surface of the sapphire window, as shown in Fig. 4. The image does not represent a clear evidence of this phenomenon, and specific analytical experiments are required to quantify the molecular mass and the nature of the extracted material. Nevertheless, it is evident that at the end of the foaming experiment the sapphire window loses transparency, as a consequence of the presence of traces of material.

3.3. Pressure drop history

PDR is of key importance in foaming because it influences the thermodynamic thrust that causes phase separation. We observed a different behavior with different PBA as reported in Fig. 5a: for typical gaseous blowing agents such as CO_2, we observed a one-step reduction in pressure. For the liquid blowing agent (i.e., Methylal), we observed a two-step reduction in pressure: a fast reduction of pressure, much faster than the one-step reduction registered with CO_2, followed by a slower one. We infer that the faster *PDR* observed for the liquid case is due to the negligible compressibility: with valve opening, the volume available to the liquid increases causing an immediate pressure drop, only partially sustained by the liquid to vapor transition.

To support this thesis, in Fig. 5b we report the different pressure reduction curves of different experiments carried out at the same temperature of 132.0 °C and at different solubilization pressures, namely 30.0, 45.0 and 60.0 bar. It is interesting to note that, regardless of the set pressure, the pressure at which the slope changes is almost the same in all cases and is approximately 12 bar, which is in the vicinity of the vapor pressure of Methylal at the test temperature ($p = 10.9$ bar, $T = 135.0$ °C). Furthermore, the second slope remains the same for all experiments, with a value of 0.44 bar/s. The advantages of a structured pressure drop was demonstrated in several works, however, this is usually difficult to obtain because it requires complex control systems [54,55]. On the other hand, we were able to obtain a double slope pressure drop by just exploiting the phase transition of the blowing agent, which is of great potential in foaming.

3.4. Liquid-vapor foaming

This technique does not allow high pressures to be reached and the pellets do not foam until at least 6.5 bar are reached. Since the solubility is high enough under ambient conditions to provide formation of gas bubbles, the failure of these foaming attempts is probably due to low *PDR* (less than 18.7 bar/s). Moreover, since the system only works at equilibrium, temperature and pressure are always coupled, and it is more difficult to study the effects of all parameters separately. No data will be reported on these foams due to negligible attained density reduction.

3.5. Liquid foaming

The effect of process parameters on the outcomes of liquid foaming experiments are here presented. Parameters of interest in this

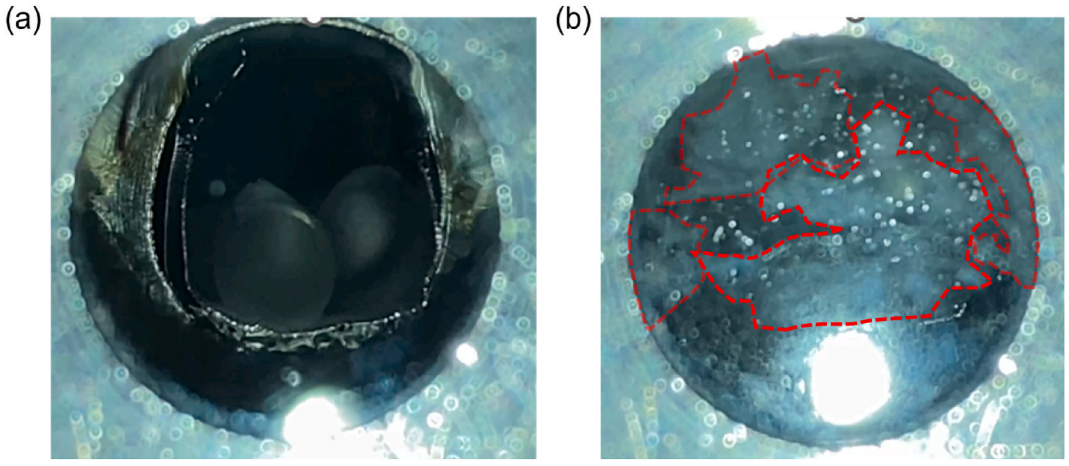

Fig. 4. Pictures of the sapphire window taken before (a) and after (b) foaming. Traces of material are visible on the glass surface in figure (b) as marked by the red dashed outline.

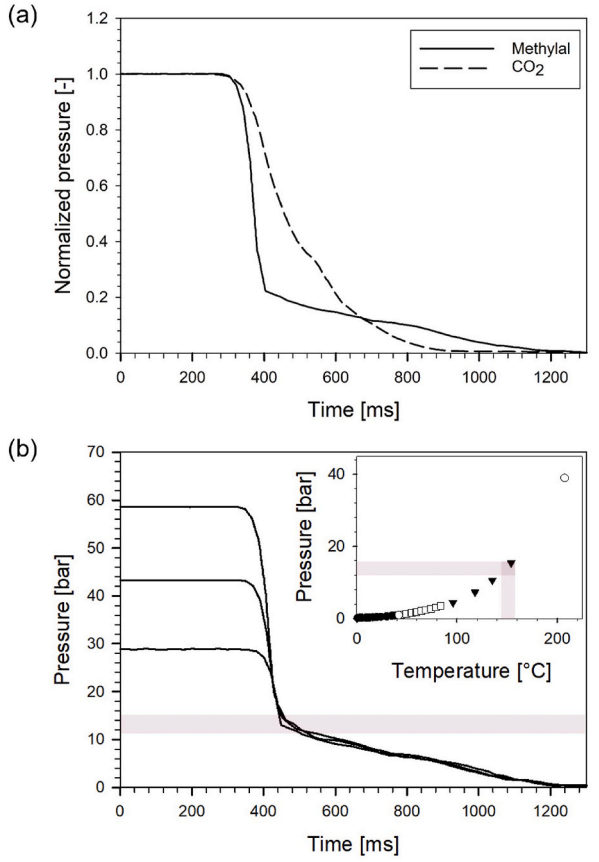

Fig. 5. (a) Pressure (normalized by the solubilization pressures) reduction curves in foaming experiments with gaseous blowing agent (dashed line) and liquid blowing agent (solid line) and (b) pressure reduction curves of liquid foaming experiments alone at different values of solubilization pressures (in the inset, Fig. 3 is reproduced for proper comparison).

study were temperature, gas concentration (here, equivalently, solubilization pressure, as we designed the foaming process to achieve uniform gas concentration), and *PDR*. The results are given in terms of the density and morphology of the final product.

First, we examined the effect of temperature at a fixed pressure of 45.0 bar, and a variable *PDR* (Fig. 6a). As it can be seen in Fig. 7a, the density decreases as the temperature increases until, at approximately 135.0 °C, a minimum of 352 kg/m^3 is reached, which is

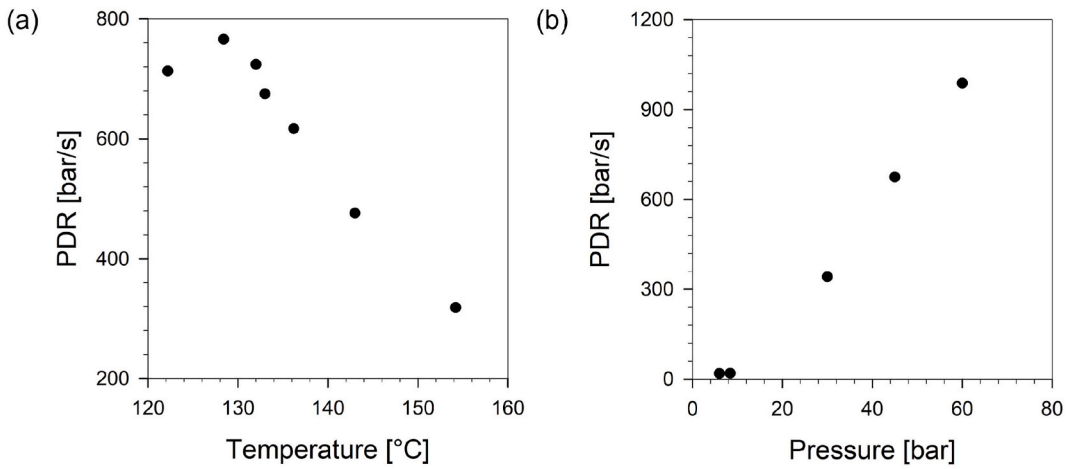

Fig. 6. *PDR* measurements: (a) effect of foaming temperature, at a constant solubilization pressure of 45.0 bar; (b) effect of pressure, at a constant foaming temperature of 132.0 °C.

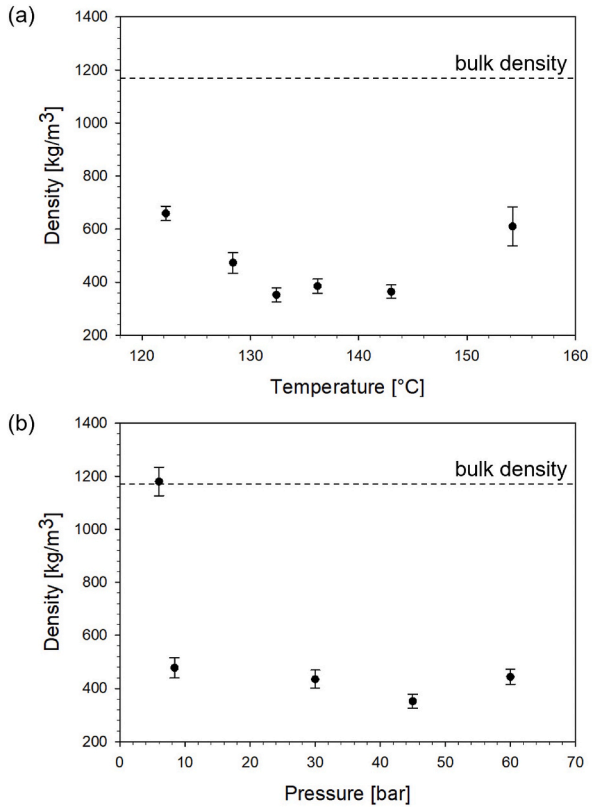

Fig. 7. Effect of temperature (a) and pressure (b) on the mean density of TPU foamed by the liquid foaming technique.

slightly larger than the one produced with a similar technology by Hossieny et al. [25]. Above 135.0 °C the viscosity reduction induces the foam collapse, resulting in the rise of the density [8]. The available foaming temperature window at 45.0 bar is between 123.4 °C and 143.0 °C.

Then, we studied the effect of pressure at a fixed temperature of approximately 132.0 °C and at a variable *PDR*, depending on the maximum pressure value (Fig. 6b). The results are shown in Fig. 7b. We can see that, at pressures lower than 6.0 bar and *PDR*s lower than 18.7 bar/s, foaming does not occur, confirming the results obtained with the first approach to the liquid foaming method (see subsection 3.4). At higher pressures, the density is noticeably reduced, reaching values comparable to those obtained in the temperature sweep experiments. This can also be connected to the fact that a higher *PDR* can be reached at higher foaming pressures, which would confirm the importance of the *PDR* in inducing foaming. The morphology of the foamed samples under the different foaming conditions is shown in Figs. 8 and 9.

As it is visible, the TPU beads (five, in a typical experiment, see section 2.2) weld together at foaming in these experimental conditions. Regardless of the low quality of the images, the influence of the process parameters is clear and consistent with the density measurements. When the pressure is lower than 6 bar and the *PDR* is lower than 18.7 bar/s, foaming does not occur, while, at higher *PDR*, foaming begins to occur (Fig. 9d-e-f). The foamed product shows a very coarse morphology with a large fraction of large bubbles and a small fraction of smaller bubbles. As pressure increases, the bubbles seem to get smaller in dimension. Indeed, the color of the foam fades towards white as a hint to the reduction of the bubble diameter.

It is worth noticing that in all cases (full temperature and pressure ranges) the bubble and samples shape is not well defined. This is probably due to the high solubility of Methylal in TPU and consequent high expansion followed by extreme bubble coalescence and collapse of the entire foam. This peculiar behavior can be addressed to the effects of Methylal on TPU, described in subsection 2.7. Indeed, the very high solubility and subsequent swelling are linked to an increase in the mobility of the HS chains in TPU, which is in turn responsible for an increased foaming ability [25]. When excessive, this increase in chain mobility, and subsequent decrease in viscosity, will facilitate the bubble coalescence and collapse [56,57]. To avoid this problem, the gas foaming technique with Methylal as the co-blowing agent was performed, as fully described in Section 3.6.

3.6. Gas foaming with Methylal as a co-blowing agent

Gas foaming experiments with Methylal as a co-blowing agent were performed to reduce the amount of Methylal within the TPU beads and thus prevent the collapsed morphology typical of liquid foaming experiments. CO_2 was used as gaseous BA in a mixture with liquid Methylal. All experiments were carried out under the same temperature and *PDR* conditions ($T = 80.0$ °C and $PDR = 500$ bar/s),

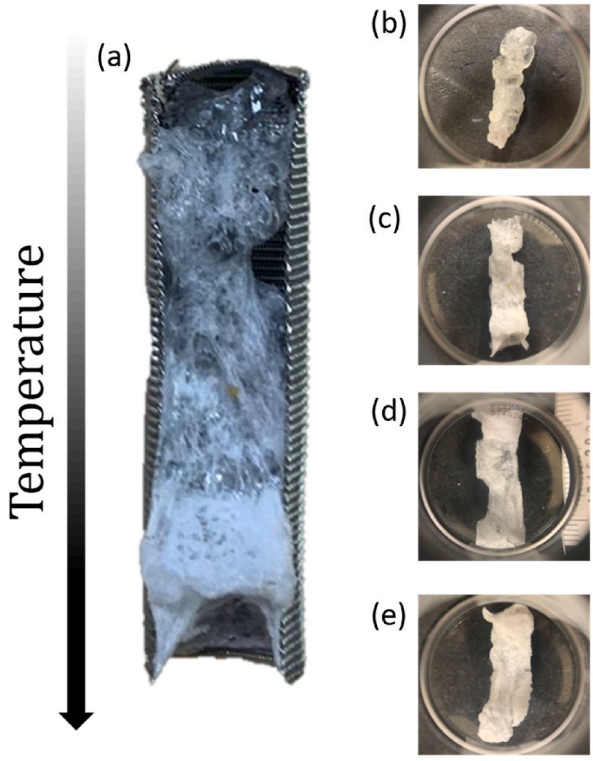

Fig. 8. Morphology of the foamed TPU beads at constant pressure (p = 45.0 bar) and with varying temperature: (b) 122.2 °C, (c) 128.4 °C, (d) 132.0 °C and (e) 136.2 °C. Picture (a) is a larger-magnification copy of picture (c) and shows the sample with a varying morphology from top to bottom. This has been related to a minor varying temperature inside the vessel.

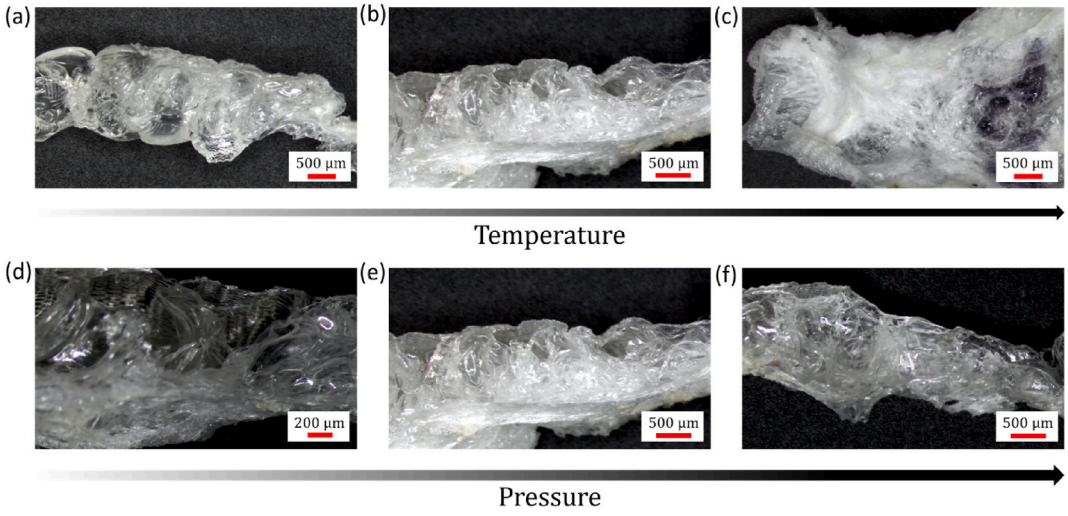

Fig. 9. Morphology of the foamed beads at the end of the liquid foaming experiments performed at constant pressure p = 45.0 bar and temperature (a) T = 120.0 °C, (b) T = 136.0 °C and (c) T = 150.0 °C. Morphology of the foamed beads at the end of the liquid foaming experiments performed at constant temperature T = 133.0 °C and pressure (d) p = 30.0 bar, (e) p = 45.0 bar and (f) p = 60.0 bar.

while pressure was changed from 40 to 120 bar to understand its effect on the final foamed product. The final foamed products were very different from those obtained with the liquid foaming technique. Indeed, beads welding does not occur; on the contrary, they stay separated and they also show a noticeably increase in volume.

The effect of pressure on the final foamed products in terms of the resulting density is shown in Fig. 10 (blue symbols). As we can see, as the pressure increases, the density of the foam decreases. The same study was carried out with Methylal and CO_2 alone as BAs

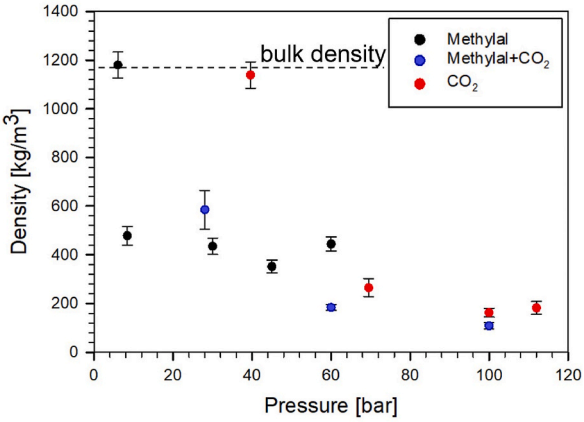

Fig. 10. Density of foamed TPU beads at different values of foaming pressures and with different blowing agents: Methylal (black , Methylal + CO_2 (blue) and CO_2 (red).

and the results are compared in Fig. 10 (black and red symbols, respectively). The minimum density value reached with CO_2 alone is 163 kg/m^3, which is in agreement with the CO_2 blown TPU foams reported by Jun et al. [58]. It is visible that the technique that uses CO_2 and Methylal as co-blowing agents is superior to gas foaming with CO_2 alone and liquid foaming with Methylal alone. In fact, this technique ensures the lowest final densities at almost every pressure value, with a minimum density of 110 kg/m^3, so a reduction of almost 40% compared to samples foamed with CO_2 alone. Furthermore, when using the mixture, the process parameters window is broadened, allowing foaming at lower pressures, as in the case of Methylal alone. The lowest densities are obtained with the CO_2/Methylal mixture and prove that adding Methylal induces an increase of BA availability with respect to CO_2 alone. The morphology of the beads foamed with the CO_2/Methylal mixture was studied and is shown in Fig. 11.

This morphology appears to be significantly different from the morphology of the beads foamed with the liquid foaming technique (Fig. 9). The bubbles are smaller in dimension. Moreover, the bubble walls are well defined, and neither buckling, nor collapse occur. In general, this technique significantly improves foam morphology compared to the liquid foaming technique. The presence of a large boundary region is detected in which the bubbles appear larger in dimension and less dense (Fig. 11a). This probably occurs because of the partial escape of Methylal during CO_2 sorption [59]. Comparison with the morphology of CO_2-only foamed TPU beads confirms this hypothesis (Fig. 11b). Further studies on Methylal diffusivity in TPU could improve our understanding of dense skin formation [60]. When CO_2 is the sole PBA, the bubbles are larger in dimension and less dense, with a more defined bubble wall, just as they appear in the boundary region of Fig. 11c–d.

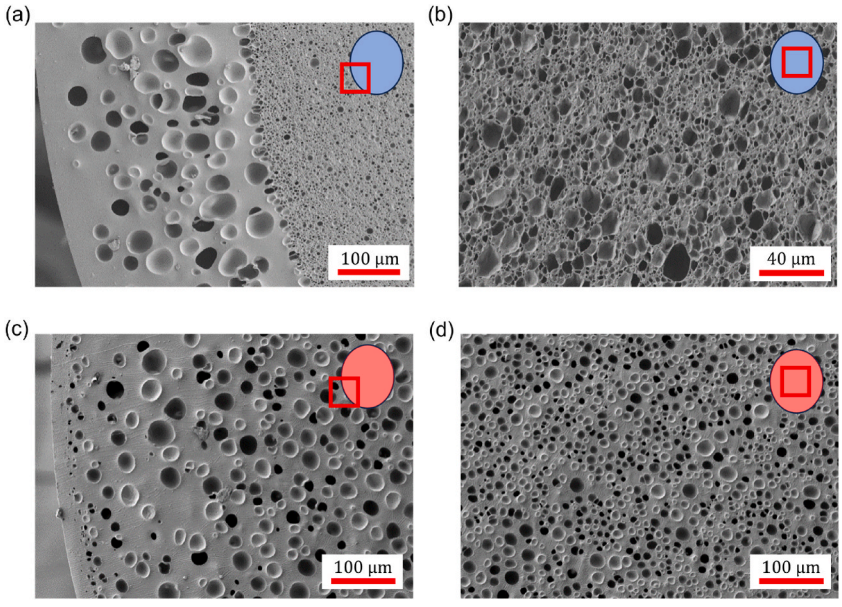

Fig. 11. Morphology of TPU beads after the gas foaming experiment with the CO_2/Methylal mixture (a,b) and with CO_2 alone (c,d) as the PBA. Pictures are taken at the center of the foamed beads (b,d) and on the boundary (a,c).

4. Conclusions

Methylal proved to be an excellent physical blowing agent for TPU. It has a very high solubility in the polymer of interest and thus causes a large swelling of the polymer pellets due to an enhancement in chain mobility. Additionally, a strong plasticizing effect and a low molecular weight fraction extraction from TPU were detected.

When used alone, in its liquid state, a non-trivial pressure drop reduction is detected, caused by the occurrence of phase transition. This proves that a complex pressure reduction can be obtained by simply exploiting the nature of the BA rather than using a regulation system. However, the resulting foamed samples display moderate densities (i.e., 400 kg/m^3) with collapsed morphologies, probably due to the extremely high Methylal solubility and swelling ability.

When used in combination with other gaseous blowing agents, namely CO_2, improved results are obtained. The densities of the foamed samples are lower than those reached with the liquid foaming technique (110 kg/m^3 vs. the above mentioned 400 kg/m^3), and the morphologies do not show collapse. As seen from the SEM images, bubbles are smaller in dimension and a boundary region is detected.

The results achieved with the combination of the two blowing agents are also better than those obtained with gaseous blowing agents alone, namely CO_2, both in terms of final density and foaming window, which means that Methylal highly enhances the foaming ability of CO_2 and could be of help in industrial practices.

Overall, Methylal is applicable in foaming technologies, but further studies would enhance the understanding of its role as a blowing agent.

Data availability

The data that support the findings of this study are available on request from the corresponding author, E.D.M.

CRediT authorship contribution statement

Lorenzo Miele: Writing – review & editing, Writing – original draft, Validation, Methodology, Investigation, Formal analysis, Data curation, Conceptualization. **Emilia Di Lorenzo:** Writing – review & editing, Writing – original draft, Validation, Methodology, Investigation, Formal analysis, Data curation, Conceptualization. **Céline Guissart:** Writing – review & editing, Supervision, Conceptualization. **Ernesto Di Maio:** Writing – review & editing, Writing – original draft, Supervision, Investigation, Formal analysis, Conceptualization.

Declaration of competing interest

The authors declare that they have no known competing financial interests or personal relationships that could have appeared to influence the work reported in this paper.

References

[1] J.W. Boretos, W.S. Pierce, Segmented polyurethane: a new elastomer for biomedical applications, Science 158 (3807) (1967) 1481–1482.
[2] B. Lan, P. Li, Q. Yang, P. Gong, Dynamic self-generation of hydrogen bonding and relaxation of polymer chain segment in stabilizing thermoplastic polyurethane microcellular foams, Mater. Today Commun. 24 (2020) 101056.
[3] A. Frick, A. Rochman, Characterization of TPU-elastomers by thermal analysis (DSC), Polym. Test. 23 (4) (2004) 413–417.
[4] G. Holden, Thermoplastic elastomers, in: Applied Plastics Engineering Handbook, Elsevier, 2011, pp. 77–91.
[5] G. Wang, G. Wan, J. Chai, B. Li, G. Zhao, Y. Mu, C.B. Park, Structure tunable thermoplastic polyurethane foams fabricated by supercritical carbon dioxide foaming and their compressive mechanical properties, J. Supercrit. Fluids 149 (2019) 127–137.
[6] E. Christenson, J. Anderson, A. Hiltner, Biodegradation mechanisms of polyurethane elastomers, Corrosion Engineering, Sci. Technol. 42 (4) (2007) 312–323.
[7] M.F. Ahmed, Y. Li, Z. Yao, K. Cao, C. Zeng, TPU/PLA blend foams: enhanced foamability, structural stability, and implications for shape memory foams, J. Appl. Polym. Sci. 136 (17) (2019) 47416.
[8] E. Di Maio, S. Iannace, G. Mensitieri, Foaming with Supercritical Fluids, Elsevier, 2021, pp. 21–32.
[9] P. Krol, Synthesis methods, chemical structures and phase structures of linear polyurethanes. properties and applications of linear polyurethanes in polyurethane elastomers, copolymers and ionomers, Prog. Mater. Sci. 52 (6) (2007) 915–1015.
[10] M. Ates, S. Karadag, A.A. Eker, B. Eker, Polyurethane foam materials and their industrial applications, Polym. Int. 71 (10) (2022) 1157–1163.
[11] H.A. Kharbas, J.D. McNulty, T. Ellingham, C. Thompson, M. Manitiu, G. Scholz, L.-S. Turng, Comparative study of chemical and physical foaming methods for injection-molded thermoplastic polyurethane, J. Cell. Plast. 53 (4) (2017) 373–388.
[12] W. Zhai, J. Jiang, C.B. Park, A review on physical foaming of thermoplastic and vulcanized elastomers, Polym. Rev. 62 (1) (2022) 95–141.
[13] D. Raps, N. Hossieny, C.B. Park, V. Altstädt, Past and present developments in polymer bead foams and bead foaming technology, Polymer 56 (2015) 5–19.
[14] M. Sauceau, J. Fages, A. Common, C. Nikitine, E. Rodier, New challenges in polymer foaming: a review of extrusion processes assisted by supercritical carbon dioxide, Prog. Polym. Sci. 36 (6) (2011) 749–766.
[15] K. Taki, D. Kitano, M. Ohshima, Effect of growing crystalline phase on bubble nucleation in poly (l-lactide)/CO_2 batch foaming, Ind. Eng. Chem. Res. 50 (6) (2011) 3247–3252.
[16] C.B. Park, A.H. Behravesh, R.D. Venter, Low density microcellular foam processing in extrusion using co2, Polym. Eng. Sci. 38 (11) (1998) 1812–1823.
[17] A.K. Bledzki, H. Kirschling, M. Rohleder, A. Chate, Correlation between injection molding processing parameters and mechanical properties of microcellular polycarbonate, J. Cell. Plast. 48 (4) (2012) 301–340.
[18] C. Ge, Q. Ren, S. Wang, W. Zheng, W. Zhai, C.B. Park, Steam-chest molding of expanded thermoplastic polyurethane bead foams and their mechanical properties, Chem. Eng. Sci. 174 (2017) 337–346.
[19] Z. Guo, A.C. Burley, K.W. Koelling, I. Kusaka, L.J. Lee, D.L. Tomasko, Co2 bubble nucleation in polystyrene: experimental and modeling studies, J. Appl. Polym. Sci. 125 (3) (2012) 2170–2186.

[20] C.B. Park, D.F. Baldwin, N.P. Suh, Effect of the pressure drop rate on cell nucleation in continuous processing of microcellular polymers, Polym. Eng. Sci. 35 (5) (1995) 432–440.
[21] K. Taki, Experimental and numerical studies on the effects of pressure release rate on number density of bubbles and bubble growth in a polymeric foaming process, Chem. Eng. Sci. 63 (14) (2008) 3643–3653.
[22] E. Di Maio, G. Mensitieri, S. Iannace, L. Nicolais, W. Li, R. Flumerfelt, Structure optimization of polycaprolactone foams by using mixtures of co2 and n2 as blowing agents, Polym. Eng. Sci. 45 (3) (2005) 432–441.
[23] R. Li, J.H. Lee, C. Wang, L.H. Mark, C.B. Park, Solubility and diffusivity of co2 and n2 in TPU and their effects on cell nucleation in batch foaming, J. Supercrit. Fluids 154 (2019) 104623.
[24] C. Ge, S. Wang, W. Zheng, W. Zhai, Preparation of microcellular thermoplastic polyurethane (TPU) foam and its tensile property, Polym. Eng. Sci. 58 (S1) (2018) E158–E166.
[25] N.J. Hossieny, M.R. Barzegari, M. Nofar, S.H. Mahmood, C.B. Park, Crystallization of hard segment domains with the presence of butane for microcellular thermoplastic polyurethane foams, Polymer 55 (2) (2014) 651–662.
[26] R. Gendron, M.F. Champagne, Y. Delaviz, M.E. Polasky, Foaming polystyrene with a mixture of co2 and ethanol, J. Cell. Plast. 42 (2) (2006) 127–138.
[27] A. Salerno, U. Clerici, C. Domingo, Solid-state foaming of biodegradable polyesters by means of supercritical CO_2/ethyl-lactate mixtures: towards designing advanced materials by means of sustainable processes, Eur. Polym. J. 51 (2014) 1–11.
[28] I. Tsivintzelis, E. Pavlidou, C. Panayiotou, Biodegradable polymer foams prepared with supercritical co2–ethanol mixtures as blowing agents, J. Supercrit. Fluids 42 (2) (2007) 265–272.
[29] L.E. Daigneault, R. Gendron, Blends of co2 and 2-ethyl hexanol as replacement foaming agents for extruded polystyrene, J. Cell. Plast. 37 (3) (2001) 262–272.
[30] N. Zhao, L.H. Mark, C. Zhu, C.B. Park, Q. Li, R. Glenn, T.R. Thompson, Foaming poly (vinyl alcohol)/micro-fibrillated cellulose composites with CO_2 and water as co-blowing agents, Ind. Eng. Chem. Res. 53 (30) (2014) 11962–11972.
[31] C. Zhang, B. Zhu, L.J. Lee, Extrusion foaming of polystyrene/carbon particles using carbon dioxide and water as co-blowing agents, Polymer 52 (8) (2011) 1847–1855.
[32] H. Voelker, G. Alicke, H. Schuch, M. Weilbacher, R. Weber, Production of foam sheets of high compressive strength, US Patent 5 (182) (1993) 308. Jan. 26.
[33] A. Nistor, A. Rygl, M. Bobak, M. Sajfrtova, J. Kosek, Micro-cellular polystyrene foam preparation using high pressure CO_2: the influence of solvent residua, Macromol. Symp. 333 (2013) 266–272. Wiley Online Library.
[34] A. Nistor, M. Topiar, H. Sovova, J. Kosek, Effect of organic co-blowing agents on the morphology of CO_2 blown microcellular polystyrene foams, J. Supercrit. Fluids 130 (2017) 30–39.
[35] X. Lan, W. Zhai, W. Zheng, Critical effects of polyethylene addition on the autoclave foaming behavior of polypropylene and the melting behavior of polypropylene foams blown with n-pentane and CO_2, Ind. Eng. Chem. Res. 52 (16) (2013) 5655–5665.
[36] T. Tuladhar, M. Mackley, Experimental observations and modelling relating to foaming and bubble growth from pentane loaded polystyrene melts, Chem. Eng. Sci. 59 (24) (2004) 5997–6014.
[37] G. Salejova, J. Kosek, Dynamics of foaming of polystyrene particles, Macromol. Symp. 243 (2006) 233–246. Wiley Online Library.
[38] H.R. Azimi, M. Rezaei, F. Abbasi, The effect of expansion conditions on the batch foaming dynamics of st–mma copolymer, J. Cell. Plast. 48 (2) (2012) 125–140.
[39] H.R. Azimi, M. Rezaei, M. Salehi, The effect of copolymer composition on the batch foaming dynamics of styrene/methylmethacrylate copolymers, J. Thermoplast. Compos. Mater. 30 (1) (2017) 47–66.
[40] M. Salehi, M. Rezaei, M.S. Hosseini, Experimental and theoretical investigation on polystyrene/n-pentane foaming process, Int. J. Material Form. 10 (2017) 421–434.
[41] S.K. Yeh, Y.R. Chen, T.W. Kang, T.J. Tseng, S.P. Peng, C.C. Chu, S.P. Rwei, W.J. Guo, Different approaches for creating nanocellular TPU foams by supercritical co2 foaming, J. Polym. Res. 25 (2018) 1–12.
[42] Lambiotte & Cie, Products, methylal. https://www.lambiotte.com/methylal/, 2023, 2023-09-25.
[43] R. Sun, I. Delidovich, R. Palkovits, Dimethoxymethane as a cleaner synthetic fuel: synthetic methods, catalysts, and reaction mechanism, ACS Catal. 9 (2) (2019) 1298–1318.
[44] L. Wianowski, A. Bia lkowska, L. Dobrowolski, I. Zarzyka, Physical blowing agents for polyurethanes, Polimery 65 (2) (2020) 83–94.
[45] M. Kurańska, A. Prociak, S. Micha lowski, A. Zawadzińska, The influence of blowing agents type on foaming process and properties of rigid polyurethane foams, Polimery 63 (2018) 672–678.
[46] Y. Chen, D. Li, H. Zhang, Y. Ling, K. Wu, T. Liu, D. Hu, L. Zhao, Antishrinking strategy of microcellular thermoplastic polyurethane by comprehensive modeling analysis, Ind. Eng. Chem. Res. 60 (19) (2021) 7155–7166.
[47] X. Gao, Y. Chen, P. Chen, Z. Xu, L. Zhao, D. Hu, Supercritical CO_2 foaming and shrinkage resistance of thermoplastic polyurethane/modified magnesium borate whisker composite, J. CO2 Util. 57 (2022) 101887.
[48] D. Tammaro, V. Contaldi, M.G. Pastore Carbone, E. Di Maio, S. Iannace, A novel lab-scale batch foaming equipment: the mini-batch, J. Cell. Plast. 52 (5) (2016) 533–543.
[49] D. Tammaro, A. De Maio, M.G. Pastore Carbone, E. Di Maio, S. Iannace, Ps foams at high pressure drop rates, AIP Conf. Proc. 1599 (2014) 473–476. American Institute of Physics.
[50] M. Albert, I. Hahnenstein, H. Hasse, G. Maurer, Vapor- liquid and liquid- liquid equilibria in binary and ternary mixtures of water, methanol, and methylal, J. Chem. Eng. Data 46 (4) (2001) 897–903.
[51] K.A. Kobe, J.F. Mathews, Critical properties and vapor pressures of some organic nitrogen and oxygen compounds, J. Chem. Eng. Data 15 (1) (1970) 182–186.
[52] J. Lu, H. Zhang, Y. Chen, Y. Ge, T. Liu, Effect of chain relaxation on the shrinkage behavior of TPEE foams fabricated with supercritical co2, Polymer 256 (2022) 125262.
[53] C.A. Schneider, W.S. Rasband, K.W. Eliceiri, Nih image to imagej: 25 years of image analysis, Nat. Methods 9 (7) (2012) 671–675.
[54] C. Brondi, M.R. Di Caprio, G. Scherillo, E. Di Maio, T. Mosciatti, S. Cavalca, V. Parenti, M. Corti, S. Iannace, Thermosetting polyurethane foams by physical blowing agents: chasing the synthesis reaction with the pressure, J. Supercrit. Fluids 154 (2019) 104630.
[55] J.-B. Bao, T. Liu, L. Zhao, G.-H. Hu, A two-step depressurization batch process for the formation of bi-modal cell structure polystyrene foams using scco2, J. Supercrit. Fluids 55 (3) (2011) 1104–1114.
[56] K. Taki, K. Tabata, S.-i. Kihara, M. Ohshima, Bubble coalescence in foaming process of polymers, Polym. Eng. Sci. 46 (5) (2006) 680–690.
[57] D. Tammaro, G. D'Avino, E. Di Maio, R. Pasquino, M. Villone, D. Gonzales, M. Groombridge, N. Grizzuti, P. Maffettone, Validated modeling of bubble growth, impingement and retraction to predict cell-opening in thermoplastic foaming, Chem. Eng. J. 287 (2016) 492–502.
[58] L. Jun, Z. Qin, H.-Y. Mi, B.-B. Dong, C. Liua, C. Shena, Fabrication of thermoplastic polyurethane foams with wrinkled pores and superior energy absorption properties by CO_2 foaming and fast chilling, Macromol. Mater. Eng. 307 (1) (2022) 2100600.
[59] M. Trofa, E. Di Maio, P.L. Maffettone, Multi-graded foams upon time-dependent exposition to blowing agent, Chem. Eng. J. 362 (2019) 812–817.
[60] M.G. Pastore Carbone, E. Di Maio, S. Iannace, G. Mensitieri, Si-multaneous experimental evaluation of solubility, diffusivity, interfacial tension and specific volume of polymer/gas solutions, Polymer Testing 30 (3) (2011) 303–309.